

UNIVERSIDADE ESTADUAL DE CAMPINAS  
SISTEMA DE BIBLIOTECAS DA UNICAMP  
REPOSITÓRIO DA PRODUÇÃO CIENTÍFICA E INTELLECTUAL DA UNICAMP

**Versão do arquivo anexado / Version of attached file:**

Versão do Editor / Published Version

**Mais informações no site da editora / Further information on publisher's website:**

<http://www.isdsnet.com/ijds-v6n11.html>

**DOI: 0**

**Direitos autorais / Publisher's copyright statement:**

©2017 by International Society for Development and Sustainability. All rights reserved.

DIRETORIA DE TRATAMENTO DA INFORMAÇÃO

Cidade Universitária Zeferino Vaz Barão Geraldo

CEP 13083-970 – Campinas SP

Fone: (19) 3521-6493

<http://www.repositorio.unicamp.br>



# An algorithm for development of transition probabilities matrices to predicting ramp events of the global solar irradiance, based on Markov model

Hermes José Loschi \*, Yuzo Iano, Luiz Antonio F. de Sousa, Douglas Aguiar do Nascimento, Reinaldo Padilha França

*Department of Communications (DECOM), Faculty of Electrical and Computer Engineering (FEEC) at State University of Campinas (UNICAMP), Campinas, Brazil*

## Abstract

The uncertainty management is a key challenge in grid operations and the probabilistic forecasts will play an important role toward this end as the penetration of photovoltaic solar generation continues to increase. Since so many different aspects can influence in forecasting of photovoltaic solar generation, mainly for this forecasting does an intermediate step of global solar irradiance forecasting, the probabilistic forecasting to predicting ramp events is increasingly used to deal with the factor of global solar irradiance dependence of the dynamics atmospheric and presence and level of clouds, and contribute to higher prediction accuracy through characterization of the ramp events. This paper proposes an algorithm for development of transition probabilities matrices to predicting ramp events, based on Markov model, for application, mainly in the local site where there is the absence of a long amount of solarimetric dates and clouds patterns information to represent the best characteristics of the ramp events. The tests are repeated for solar data set and observations are presented, prediction modeling results with distinct properties in terms of accuracy are achieved. The results show accuracy of 7 to 20% in performance of the prediction method developed, at time intervals presented, and your discussion evidences the importance of global solar irradiance prediction methods.

**Keywords:** Uncertainty Management; Ramp-Events; Prediction

Published by ISDS LLC, Japan | Copyright © 2017 by the Author(s) | This is an open access article distributed under the Creative Commons Attribution License, which permits unrestricted use, distribution, and reproduction in any medium, provided the original work is properly cited.



**Cite this article as:** Loschi, H.J., Iano, Y., Sousa, L.A., Nascimento, D.A. and França, R.P. (2017), "An algorithm for development of transition probabilities matrices to predicting ramp events of the global solar irradiance, based on Markov model", *International Journal of Development and Sustainability*, Vol. 6 No. 11, pp. 1803-1823.

---

\* Corresponding author. E-mail address: [eng.hermes.loschi@ieee.org](mailto:eng.hermes.loschi@ieee.org)

## 1. Introduction

Among the challenges facing the world, the transition to a future of low-carbon energy through increased use of renewable energy sources is one of the most discussed priorities today. Across the world, governments are expanding their efforts to stimulate more investment in low-carbon forms of energy, especially photovoltaic solar generation. However, as the penetration of solar photovoltaic generation increases, dilemma continues to receive much attention focused on how to graciously integrate this form of unconventional and variable energy into existing power grids and eventually emerging power grids, as well as into markets. In this context, the concept of renewable forecasting addresses the fundamental task of managing uncertainty through accurate prediction of the results of solar photovoltaic generation. (Lawrence, 2014; Loschi et al., 2015; Loschi, 2017).

The variability and uncertainty of photovoltaic solar generation must be properly accounted for by the complex decision-making processes required to provide and demand equilibrium in energy systems. It is becoming increasingly clear that forecasting is a key solution for efficiently dealing with the photovoltaic solar system in the operation of the power grid, especially considering the peculiarities of this system (Naoto *et al.*, 2014; Lawrence, 2014; Loschi, 2017; Loschi et al., 2017).

A recent trend in forecasting of photovoltaic solar generation is the interest in understanding and predicting rapid changes in the power output (Kalisch and Macke, 2008; Perez et al., 2011; Huang et al., 2013; Cai et al., 2014). Such ramp events, particularly in the downward direction may create challenges for reliable power grid operations, and a ramp forecast is therefore seen as an important operational tool among some system operators of the power grids (Soares, 2014; Lopes, 2015). Ramps forecast are most relevant for the very short-term time horizon (0-6 h), hence the use of numerical weather predictions (NWP) has been of limited value for this purpose so far (Lawrence, 2014). In reality, what constitutes a significant ramp event will depend on the weather and geographic conditions of the place of interest for a photovoltaic solar generation.

Since so many different aspects can influence in forecasting of photovoltaic solar generation, mainly for this forecasting does an intermediate step of global solar irradiance forecasting, the probabilistic forecasting to predicting ramp events is increasingly used to deal with the factor of global solar irradiance dependence of the dynamics atmospheric and presence and level of clouds (Lawrence, 2014; Loschi et al., 2015; Loschi, 2017). A lot of forecast systems needs to forecasting of clouds patterns to produce a good forecast (Ehnberg and Bollen, 2005; Huang et al., 2013; Marquez and Coimbra, 2013; Tapakis and Charalambides, 2013; Jaouhari et al., 2015). On the other hand, solutions with wireless sensors networks (WSN) integrated with the forecast system have a solution to optimize the performance and energy efficiency of the devices associated with the photovoltaic solar generation and to produce a prediction, mainly if compared with statistical approach (Ji et al., 2009; Achleitner et al., 2014; Loschi et al., 2015).

Moreover, some others issues impact in the implementation of this system, as the dependence of solarimetric dates and clouds patterns information on the local site. Through our academic research, understand that in the absence of a significant amount of these dates, as periods whole one or more stations

of the year, the reliability of the prediction system result can be influenced, which results in a failure to predicting ramp events, being the main challenge to the predictability of global solar irradiance. In this context, this paper proposes an algorithm for development of transition probabilities matrices to predicting ramp events, based on Markov model. This algorithm can be useful and contribute to higher prediction accuracy and to improve the reliability of these systems, in the local site where there is the absence of a long amount of solarimetric dates and clouds patterns information, a reality of Brazilian scenario that was one of the motivations.

The paper is organized as follows. Section II presents a description of the problem associated with the incidence of global solar irradiance. Section III describes the system model based on Markov process, Section IV present the algorithm model and the Section V present a model demonstration. Finally, Section VI presents the conclusions.

## 2. Description of problem

The amount of solar radiation reaching the Earth surface is affected by the sun motion long the year and, most of all, from the geographical location in terms of latitude and elevation, as well as from the local meteorological conditions and clouds formation. The figures 1, 2 e 3 present the solar irradiation (energy radiant of the Sun, incident per unit of area, representing the integration of global solar irradiance for a specified time of one day), during every day of January 2015, for the location of the Natal city (Lat.  $-05^{\circ}, 50', 12''$  S and Log.  $-35^{\circ}, 12', 23''$  O), state of Rio Grande do Norte, Brazil. This location was taken as reference for the present study, because is part of SONDA project (National network station for data collection weather applied to the energy sector), that provide a large amount of solarimetric dates for the Brazilian territory (Martins et al., 2007).

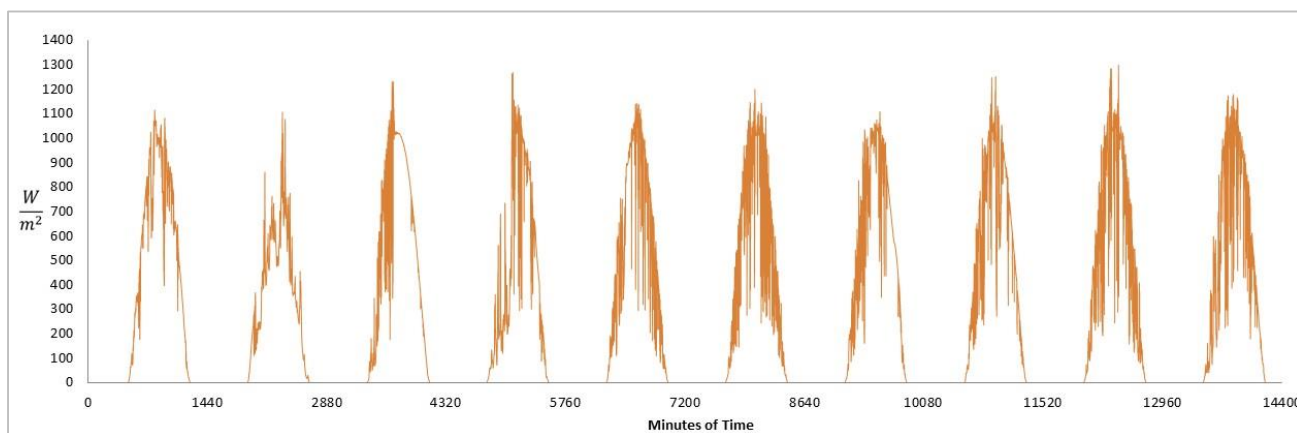


**Figure 1.** Incidence of global solar irradiance for the first period of 10 (ten) days of January 2015, Natal city

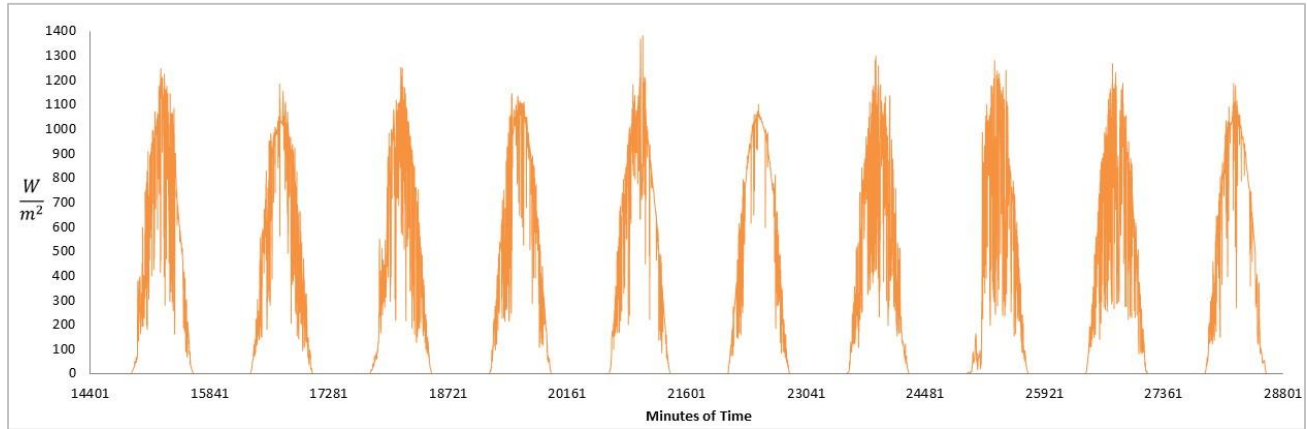


**Figure 2.** Incidence of global solar irradiance for the second period of 10 (ten) days of January 2015, Natal city.

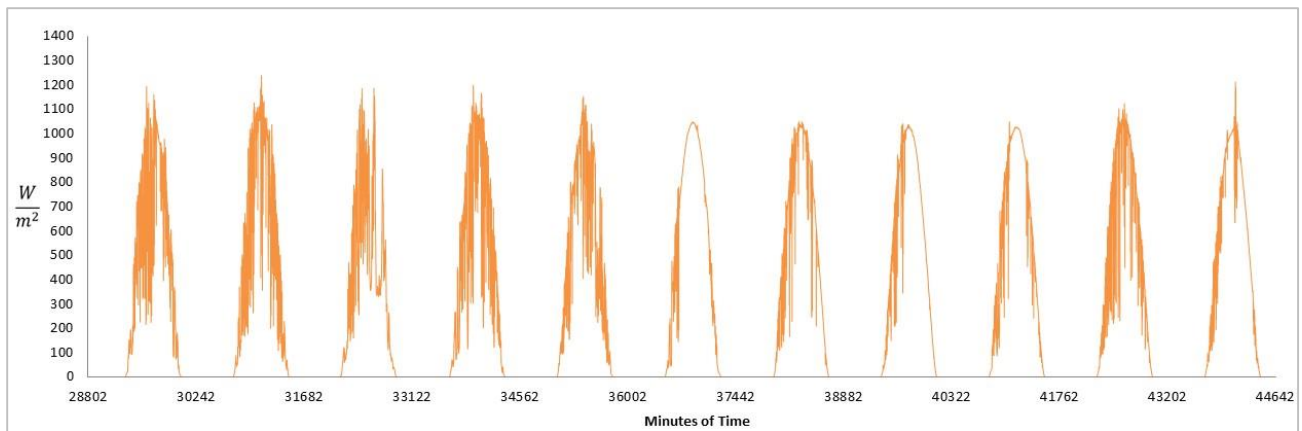


**Figure 3.** Incidence of global solar irradiance for the last period of 11 (eleven) days of January 2015, Natal city.

Accordingly, the figures 1, 2 and 3 that present the daily solar irradiation values, it is possible to calculate the solar irradiation losses between the extraterrestrial solar irradiance and the global solar irradiation values on the Earth's horizontal surface. It has been verified that these losses range between a minimum of 20 to 30% in case only atmosphere filtration, to a maximum above of 90% in case of presence of clouds. For this analysis, the daily solar irradiance ( $H$ ) dates used were from SONDA project and the extraterrestrial solar irradiance ( $H_0$ ) dates were computed as follows (Reno, et al., 2012):

$$H_0 = \frac{24}{\pi} \cdot G_{SC} \left[ 1 + 0,0033 \cos \left( \frac{360 \times n}{365} \right) \right] \times \left[ \cos \varphi \cdot \cos \delta \cdot \sin \omega_s + \frac{\pi \omega_s}{180} \cdot \sin \varphi \cdot \sin \delta \right] \quad (1)$$

where  $G_{SC}$  is the solar constant,  $n$  is the day number of the year,  $\varphi$  is latitude of the region,  $\delta$  is the solar declination angle, and  $\omega_s$  is the Sunrise hour angle. The  $\delta$  and  $\omega_s$  was computed as follows (Reno, et al., 2012):

$$\delta = 23.45 \sin \left( \frac{360(n + 284)}{365} \right) \quad (2)$$

$$\omega_s = \cos^{-1}(-\tan\varphi \cdot \tan\delta) \quad (3)$$

Through it is possible to perform statistical analysis of weather conditions based on the Clearness Index (Liu and Jordan, 1960), correlation with meteorological variables, calculate the uncertainty related to the sensors and data acquisition system, create a high-precision predictability scenario of the incidence of global solar irradiance for a specific location is a major challenge, primarily as a function of local meteorological conditions and clouds formation be different for each location. This nonconventional variable form of solar energy is the mainly responsible to uncertainty from photovoltaic solar generation, which results in a random profile of power generation. In this context, many devices associated with photovoltaic solar generation have functions that aims to dealing with this random profile of power generation, standing out the techniques of MPPT (Maximum Power Point Tracking) (Kim et al., 2001), in addition to the characteristics constructive of these devices that allow a large range of work for direct current (DC).

Moreover, even considering these techniques and characteristics constructive, the reliability of these devices, as well as the reliability of power grid operations are affected by the ramp events associated with the incidence of global solar irradiance, mainly responsible for abrupt output changes in power generation. To define a ramp event (see Figure 4), we have to determine values for its three key characteristics: direction, duration and magnitude. With respect to direction, there are two basic types of ramps: the upward ones (or ramp-up), and the downward ones (or ramp-down).

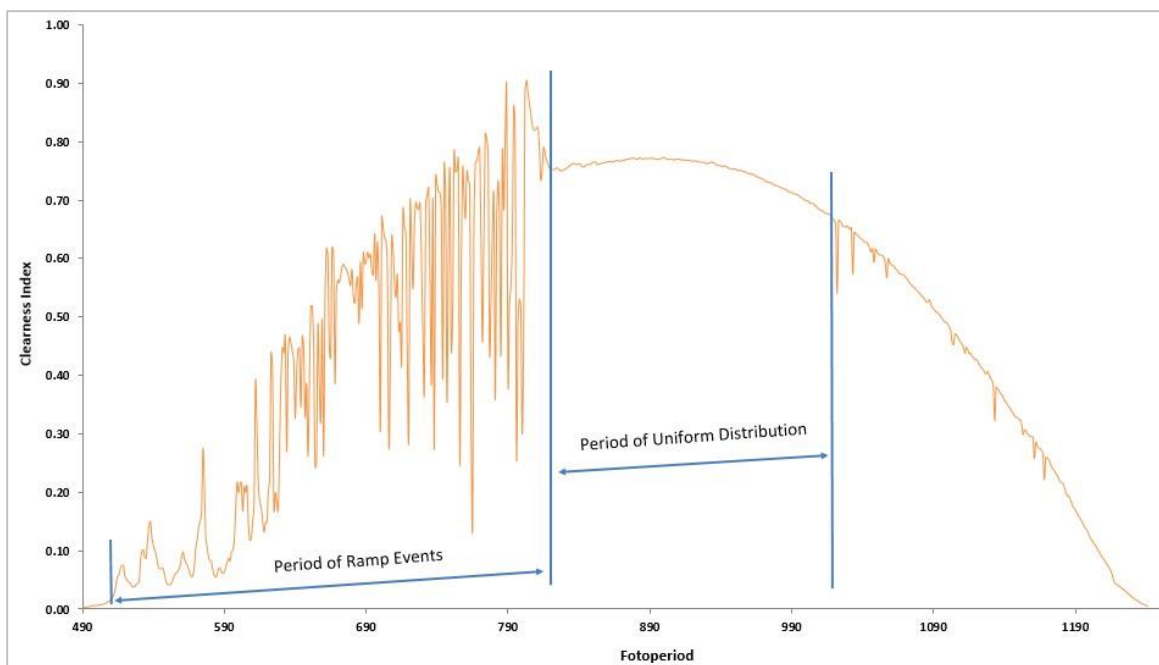


**Figure 4.** Representation of Periods of Ramp Events and Uniform Distribution

The figure 4 present the condition of the random process from ramp events associated with the incidence of global solar irradiance. Often, in a short time interval, there is a period of ramp events with different durations and magnitudes of ramp-up and ramp-down, followed by periods of uniform distribution. It is up to note that there is no a pattern for the sequence along the photoperiod to periods of ramp events and periods

of uniform distribution, how can be seen in figures 1, 2 and 3. For the photovoltaic solar generation, the ramp-up and ramp-down are due to the factor of global solar irradiance dependence of the dynamics atmospheric and presence and level of clouds, resulting in abrupt output changes in power generation. In the absence of this factor, the incidence of global solar irradiance presents a uniform distribution, and power generation follows a smooth, predictable diurnal curve as the sun moves across the sky.

Therefore, it is understood that the accuracy on the incidence of global solar irradiance prediction, consequently photovoltaic solar generation, depending on the correct characterization of the ramp events, and a recent trend to perform this characterization is the data science. However, we identified two main challenges in this field: (a) the absence of a long amount of solarimetric dates and clouds patterns information; (b) there is an of solarimetric dates and clouds patterns information availability, however, are local or regional information. In this context, probabilistic methods contribute to higher prediction accuracy through characterization of the ramp events, mainly in the local site where there is the absence of a long amount of solarimetric dates and clouds patterns information.

### 3. System model

Consider the phenomenon of ramp event and uniform distribution periods, as shown in figure 4, initially, there are two states that may be denoted by  $Y_1$  and  $Y_n$ . The specified value of  $H$  is represented by  $Y$ .

In the state  $Y_1$ , the incidence of  $H$  satisfies:

$$H \geq Y \quad (4)$$

**Definition 1.** A ramp-up event is considered to occur at time point  $t$ , the end of an interval, if the magnitude of the increase in the incidence of  $H$  is greater than the threshold value  $Y$ .

In the state  $Y_n$ , the incidence of  $H$  satisfies:

$$H < Y \quad (5)$$

**Definition 2.** A ramp-down event is considered to occur at time point  $t$ , the end of an interval, if the magnitude of the decrease in the incidence of  $H$  is greater than the threshold value  $Y$ .

In this context, some studies consider two-state Markov model (Song et al., 2013), and determine based on observations of past events (magnitude of the ramp events), a frequency that satisfaction the probabilities of transition of the state  $Y_1$  to the state  $Y_n$ . However, considering the dependence of  $H$  incidence from the dynamics atmospheric and the level and presence of clouds, the frequencies events that satisfaction the probabilities of transition of the state  $Y_1$  to the state  $Y_n$  can be endless, as represented by the Markov-process based state transition diagram, in figure 5.

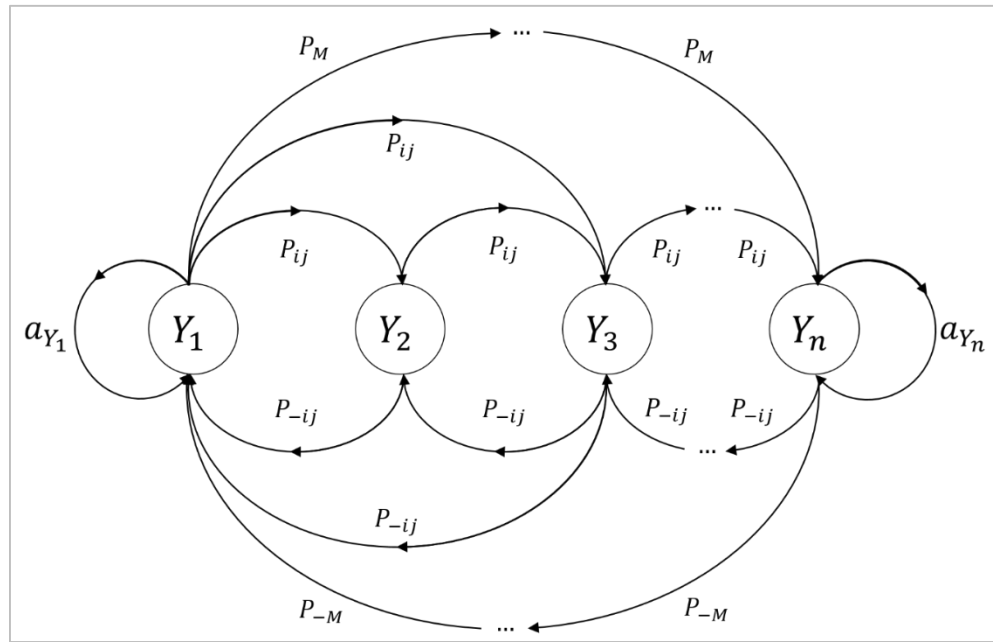


**Figure 5.** Markov-process based state transition diagram

This Markov-process based state transition diagram allows for many possible state changes, which is a closer fit to the characteristics of incidence of  $H$ . The diagram in figure 5 models the incidence of  $H$  state transition with  $M$  (determined number of possible transition from each state) transitions out of each state at each short time interval, and the  $a_{Y_1}$  and  $a_{Y_n}$  represent the probabilities of staying in states  $\#Y_1$  and  $\#Y_n$  in the next short time interval, respectively.

The transitions among states are represented by the probabilities  $P_{ij}$ , where  $ij$  represents the ramp events (ramp-up and ramp-down) associated with the incidence of  $H$  per unit time with respect to the intensity level of  $H$ . For example,  $P_{ij}$  is the transition to adjacent states involving a ramp-down associated with the incidence of  $H$  per unit time with respect to the intensity level of  $H$ , while  $P_{-ij}$  also represent transition to adjacent states, however involving a ramp-up associated with the incidence of  $H$  per unit time with respect to the intensity level of  $H$ .

The diagram in figure 5 also represents that the probabilities of transition do not occur only adjacent to the states. Therefore, the probabilities of transition are conditional to the present state of incidence of  $H$  per unit time. Consider the Markov process:

$$\begin{aligned} &P\{X(t_{k+1}) \leq x_{k+1} | X(t_k) = x_k, X(t_{k-1}) = x_{k-1}, \dots, X(t_1) = x_1, X(t_0) = x_0\} \\ &= P\{X(t_{k+1}) \leq x_{k+1} | X(t_k) = x_k\} \end{aligned} \quad (6)$$

where  $t_0 \leq t_1 \leq t_k \leq t_{k+1}$ .

The expression 6 can be understood as the conditional probability of any future event given any past event, and the present state  $X(t_k) = x_k$ , is independent of the paste event and depends only of the present state.

Therefore, the conditional probability of the expression 6 is denoted probabilities of transition and represent the state probability  $X(t_{k+1})$  to be  $x_{k+1}$  in the time interval  $t_{k+1}$  given that the state  $X(t_k)$  is  $x_k$  in the time interval  $t_k$ .

However, assuming that the unit time from of the incidence of  $H$  with respect to the intensity level of  $H$  represent a time interval of discrete time:

$$\begin{aligned} P\{X(k+1) = x_{k+1} | X(k) = x_k, X(k-1) = x_{k-1}, \dots, X(1) = x_1, X(0) = x_0\} \\ = P\{X(k+1) = x_{k+1} | X(k) = x_k\}, \quad \forall k \in \dots N \end{aligned} \quad (7)$$

The probabilities of transition  $P\{X(k+1) = x_{k+1} | X(k) = x_k\}$  represent the state probability  $X(k+1)$  to be  $x_{k+1}$  in the time interval  $k+1$  given that the state  $X(k)$  is  $x_k$  in the time interval  $k$ .

$$P\{X(k+1) = x_1 | X(k) = x_0\} = P\{X(1) = x_1 | X(0) = x_0\} \quad (8)$$

To simplify the notation, can be defined:

$$P_{ij}^n = P\{X(k+1) = j | X(k) = i\} \quad (9)$$

where  $P_{ij}^n$  are conditional probability, non-negatives, and since the process need to perform a transition to any state, the  $P_{ij}^n$  must be satisfied:

$$\sum_{j=0}^M P_{ij}^n = 1 \quad \forall \quad i; n = 0, 1, 2, \dots \quad (10)$$

A convention to represent all probabilities of transition is through the transitions probability matrix yielded by the Markov-process based state transition diagram (figure 2.1).

$$P_{ij}^n = \begin{bmatrix} P_{00}^{(n)} & P_{01}^{(n)} & \dots & P_{0M}^{(n)} \\ P_{10}^{(n)} & P_{11}^{(n)} & \dots & P_{1M}^{(n)} \\ \vdots & \vdots & \ddots & \vdots \\ P_{M0}^{(n)} & P_{M1}^{(n)} & \dots & P_{MM}^{(n)} \end{bmatrix} \quad (11)$$

The size of the matrix in (11) is  $M \times M$ , the Markov chain property that states that the sum of any row is equal to 1, and  $M$  represent the determined number of possible transition from each state, that should be represent with higher accuracy all characteristics of the ramp events.

#### 4. Algorithm model

In this section, we present the algorithm for development of transition probabilities matrices to predicting ramp events, based on Markov model. As mentioned in Section III, the value of  $M$  can be set to represent the best characteristics of the ramp events as a function of solarimetric dates and clouds patters information. However, on the other hand when there is the absence of a significant amount of these dates, as periods whole one or more stations of the year, the reliability of the prediction system result can be influenced which results in a failure to predicting ramp events.

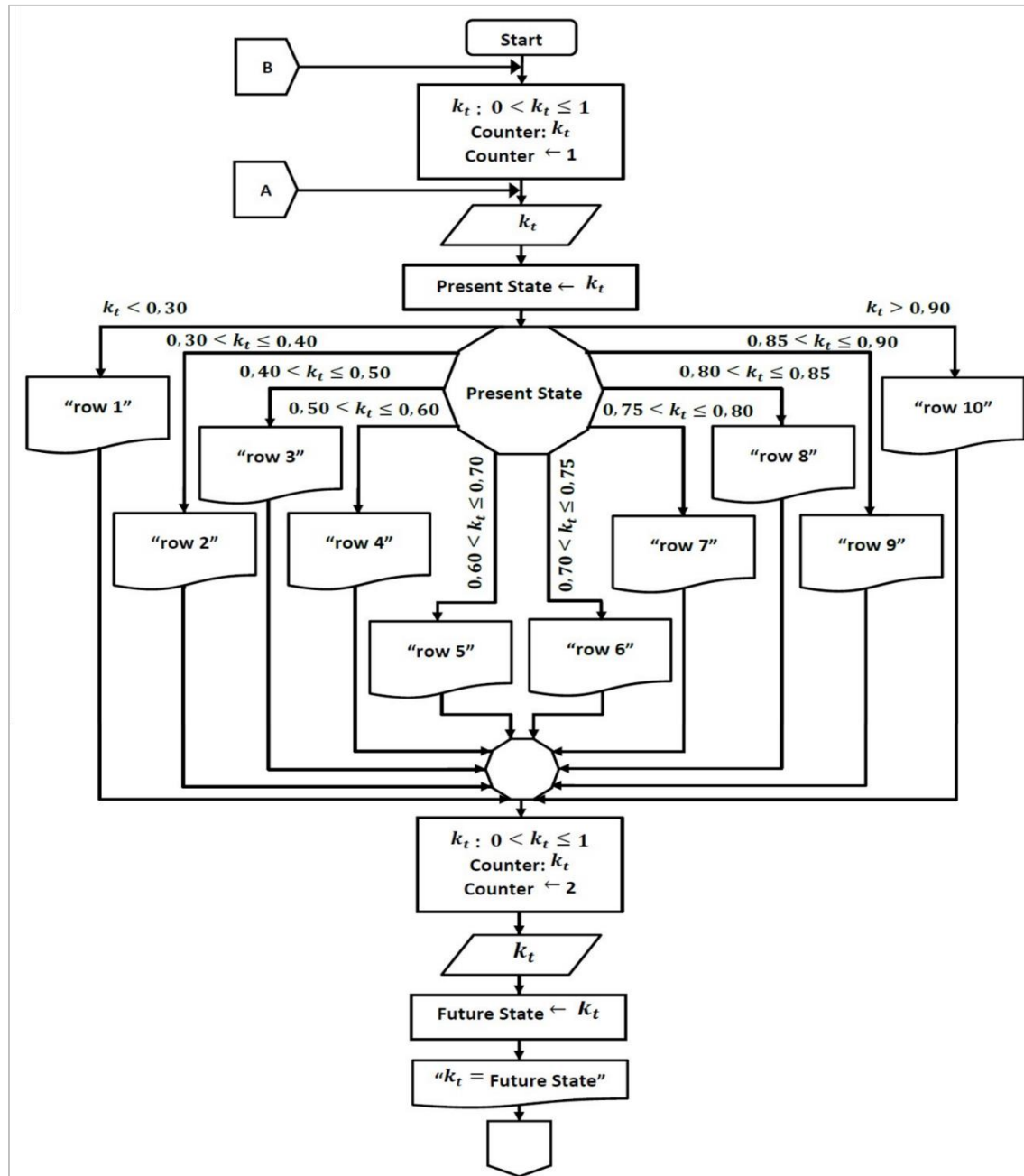


**Figure 6.a.** Flowchart of a complete calculation and selection of clearness index state to development of transition probabilities matrices

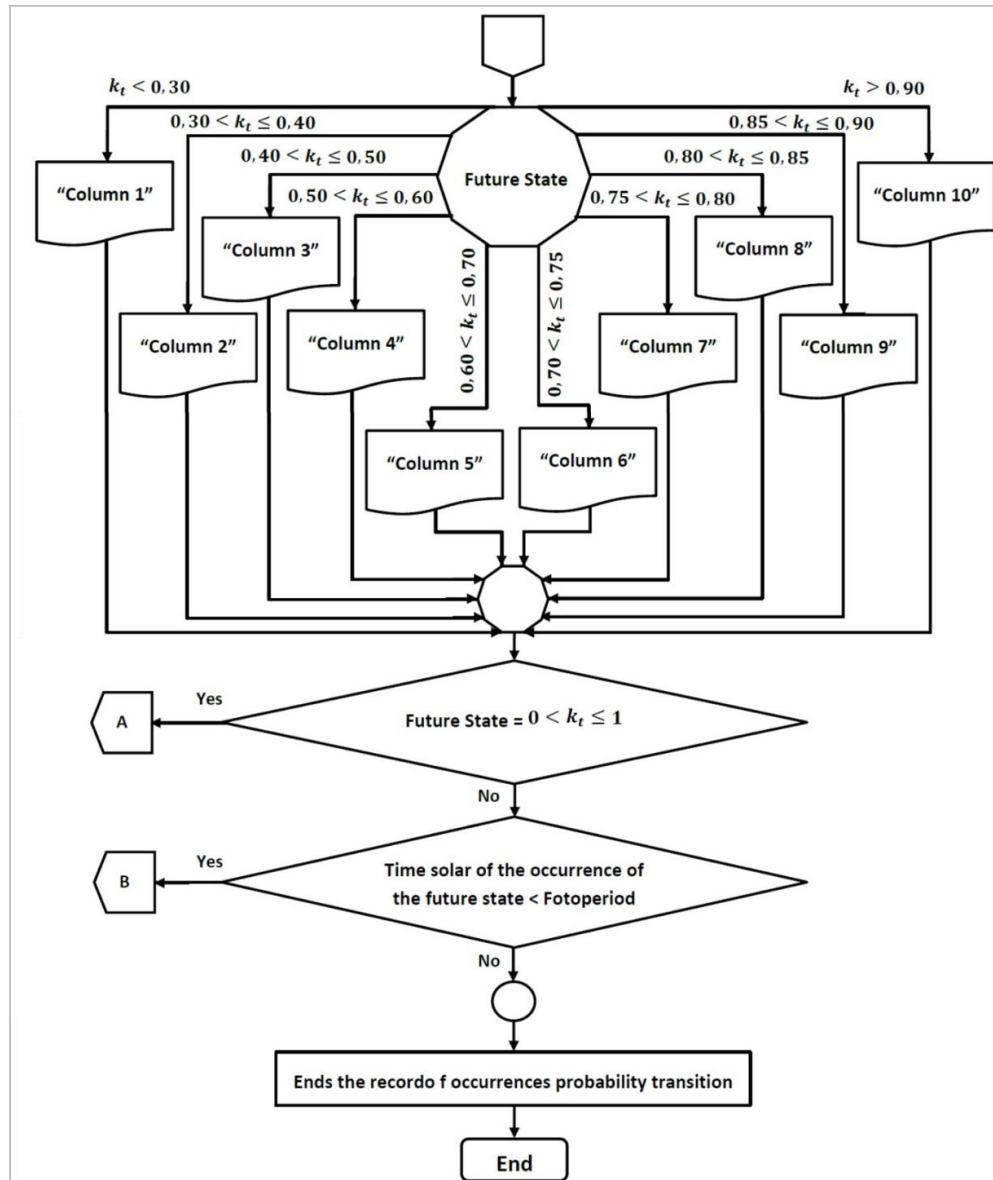


**Figure 6.b.** Flowchart of a complete calculation and selection of clearness index state to development of transition probabilities matrices

The use of the  $k_t$  is introduced to define categories of sky conditions, through the relation between the global solar irradiance and the extraterrestrial solar irradiance. Therefore, the initial premise for this algorithm development proposal, based on academic investigation carried out on the empirical solarimetric date from SONDA project, is the classification of clearness index ( $k_t$ ) in 10 (ten) state.

To perform the division of the total amplitude of the  $k_t$  in 10 (ten) state, the following interval of amplitude were adopted:  $k_t < 0,30$ ,  $0,30 \leq k_t \leq 0,40$ ,  $0,40 < k_t \leq 0,50$ ,  $0,50 < k_t \leq 0,60$ ,  $0,60 < k_t \leq 0,70$ ,  $0,70 < k_t \leq 0,80$ ,  $0,80 < k_t \leq 0,85$ ,  $0,85 < k_t \leq 0,90$ ,  $k_t > 0,90$ .

$k_t \leq 0,75$ ,  $0,75 < k_t \leq 0,80$ ,  $0,80 < k_t \leq 0,85$ ,  $0,85 < k_t \leq 0,90$  and  $k_t > 0,90$ . In addition, justify the interval of amplitude adopted by the following premises of probability distribution from state transition:

- once the present state is in one of these amplitudes, the probability of transition to a future adjacent state is most significant;
- once the present state is in one of these amplitudes, the probability of transition to a future distant state is significant;
- once the present state is in one of these amplitudes, the probability of transition to a future intermediary state is not significant;

The figure 6.a and 6.b shows the flowchart of a complete calculation and selection of clearness index ( $K_t$ ) state to development of transition probabilities matrices.

## 5. Model demonstration

In this section, to show the accuracy of the algorithm, measurements of solar irradiance with time intervals 1 (one) minutes from the Campo-Grande city (Lat.  $-20^\circ, 26', 18''$  S and Log.  $-54^\circ, 32', 18''$  O), state of Mato Grosso do Sul, Brazil, during every day of January 2014, were used to transition probabilities matrices development. The algorithm was implemented in MatLab, and the robustness of transition probabilities matrix was tested using different data from the Natal city (Lat.  $-05^\circ, 50', 12''$  S and Log.  $-35^\circ, 12', 23''$  O), state of Rio Grande do Norte, Brazil, during January 2015 and 2016. The data are obtained from SONDA project, considering the days with an occurrence of ramp events (Martins et al., 2007).

$$P_{ij}^n = \begin{bmatrix} 000 & 000 & 000 & 000 & 000 & 000 & 000 & 050 & 900 & 050 \\ 100 & 100 & 100 & 100 & 100 & 100 & 100 & 100 & 100 & 100 \\ 000 & 040 & 020 & 040 & 060 & 180 & 260 & 200 & 100 & 100 \\ 000 & 018 & 048 & 076 & 076 & 139 & 139 & 266 & 215 & 023 \\ 000 & 000 & 000 & 083 & 000 & 167 & 167 & 250 & 333 & 000 \\ 000 & 060 & 040 & 055 & 040 & 025 & 165 & 220 & 300 & 095 \\ 000 & 000 & 120 & 000 & 057 & 028 & 310 & 210 & 205 & 070 \\ 000 & 060 & 030 & 000 & 060 & 040 & 360 & 150 & 240 & 060 \\ 000 & 000 & 000 & 031 & 000 & 105 & 138 & 226 & 330 & 170 \\ 000 & 000 & 000 & 150 & 000 & 000 & 000 & 150 & 600 & 100 \end{bmatrix} \quad (12)$$

In the first step, the data are preprocessed. In this step, solar irradiation data bigger than extraterrestrial solar irradiation (i.e. data are evaluated as erroneous recording that may be caused by an unexpected event) are interpolated. The choice to work with data from a period of months is given as a function they are the dates interrupts periods, for the others locations of the SONDA project (Martins et al., 2007) there are missing data. Therefore, the proportion of the whole interpolated data was not more than 0.02% of all used data. Second, the data of Campo-Grande city with time intervals 1 (one) minutes during January 2014 are used according to demonstrated in Section IV to development of transition probabilities matrices. The equation 12 present the proposed matrix.

Once consolidated the transition probabilities matrix, the same can be used by the several methods predictions available in the literature. To this present study, the prediction approach used as a reference to the test of the transition probabilities matrix, equation 12, has reference in the method developed by (Aguar and Collares-Pereira, 1992). The figure 7 presents the block diagram of prediction calculation process.

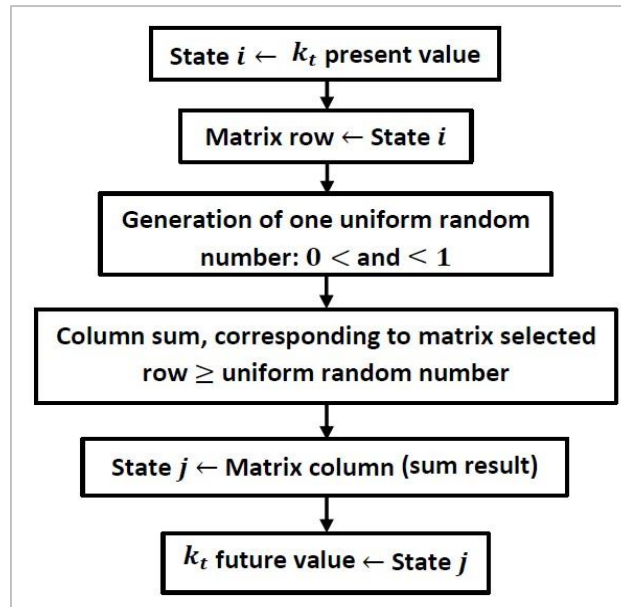


**Figure 7.** Block diagram of prediction calculation process

Therefore, the robustness of transition probabilities matrix is tested using data from the Natal city with time intervals 1 (one) minutes during January 2015 and January 2016. The main purpose of this test is based on data past (since we do not have a communication and sensing infrastructure, condition discussed in Section VI), represent the present state of  $k_t$ , to quantify the prediction approach performance based on transition probabilities matrix (equation 12), in the future time intervals 1 (one) minute (less time interval registered by the solarimetric data set of SONDA project).

The solarimetric station of Natal city, in the state of Rio Grande do Norte, has one of largest incidence index of  $H$  between all solarimetric station of SONDA project, being ideal for attest the accuracy of prediction approach in short time intervals with ramp events occurrences. The solarimetric station of Natal city, also were choice as a function to meet the criteria for treatment of solarimetric data normalized by the Baseline Surface Radiation Network - BSRN.

The comparison between the parameters (calculated and predicted value of  $k_t$ ), allow to know the prediction error, consequently the robustness of the transition probabilities matrix (equation 12). To evaluate the prediction performance are calculated parameters that quantify the degree of similarity between the calculated and predicted value of  $k_t$ , through the Root Mean Square Error -RMSE, equation 13.

$$RMSE = \sqrt{\frac{1}{n} \sum (k'_t - k_t)^2} \quad (13)$$

where  $k'_t$  is the predicted value,  $k_t$  is the calculated value and  $n$  is the number of prediction carried out.

The RMSE is a measure of precision, because, as raises squared the difference between the values is more sensitive to present the difference between the values. The value of result equal to zero indicates a perfect prediction and this value of result increases as the difference between the of calculated and predicted value also increases.

### 5.1. Tests for January 2015, Nata city data set.

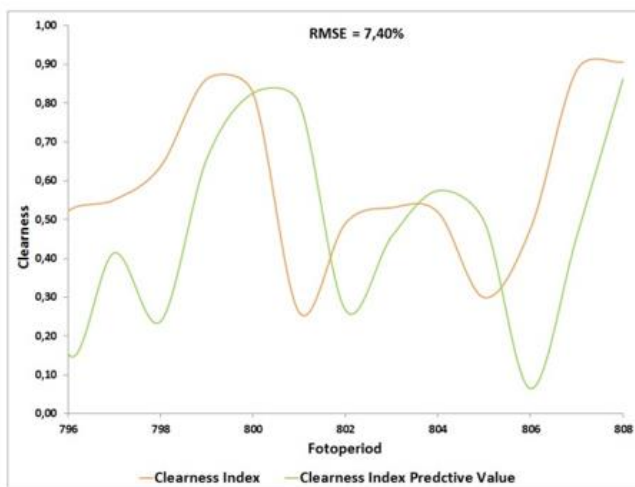


Figure 8. Ramp event occurrence - 03 January 2015

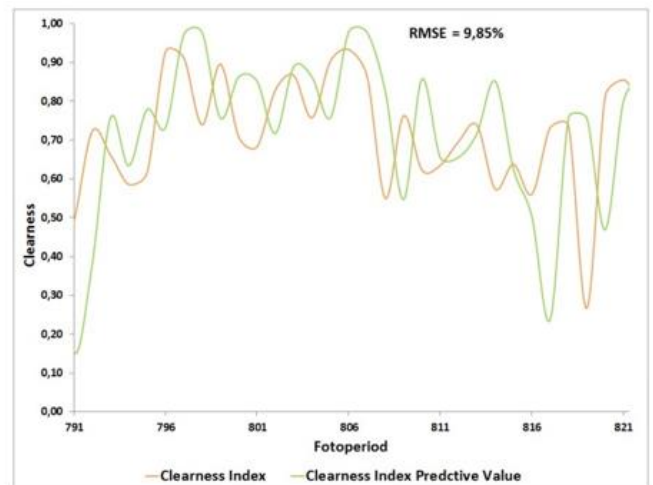


Figure 9. Ramp event occurrence - 04 January 2015

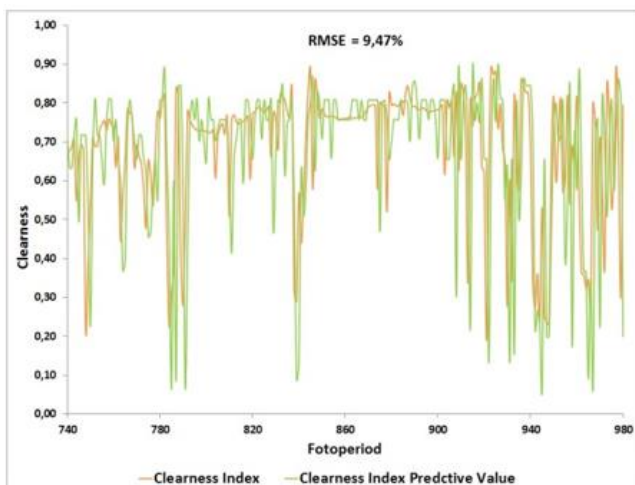


Figure 10. Ramp event occurrence - 06 January 2015

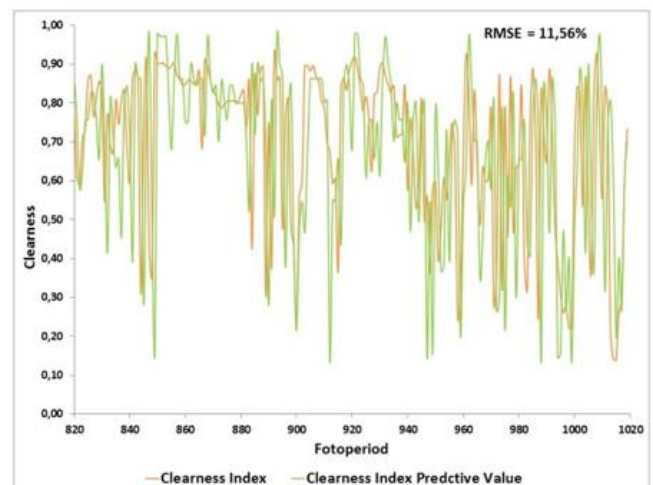


Figure 14. Ramp event occurrence - 11 January 2015

The prediction approach was implemented in MatLab, according to figures 8 to 23. The test for the days 01, 02, 05, 07, 12, 14, 16, 20, 21, 25, 26, 27, 28, 29 e 30 will not be presented as a function of the incidence profile of  $H$  have assumed a uniform distribution non-presenting the ramp events occurrences.

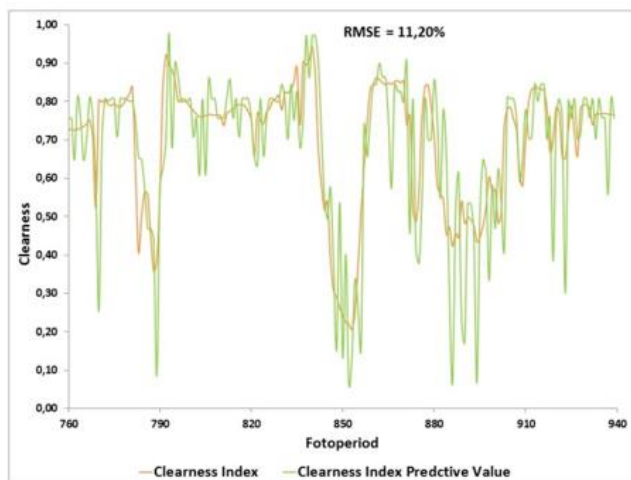


Figure 11. Ramp event occurrence - 08 January 2015

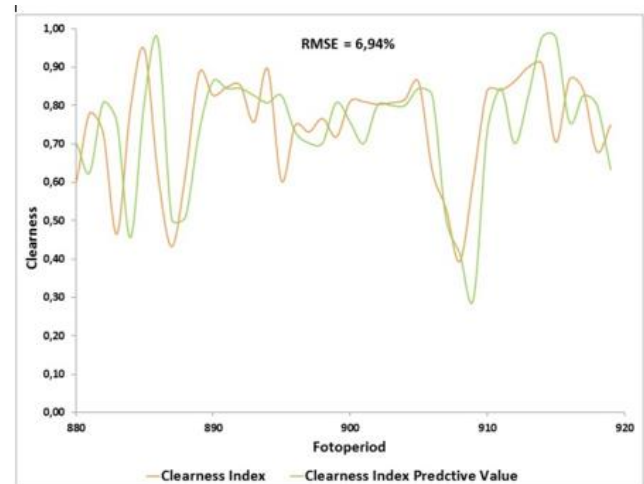


Figure 15. Ramp event occurrence - 13 January 2015

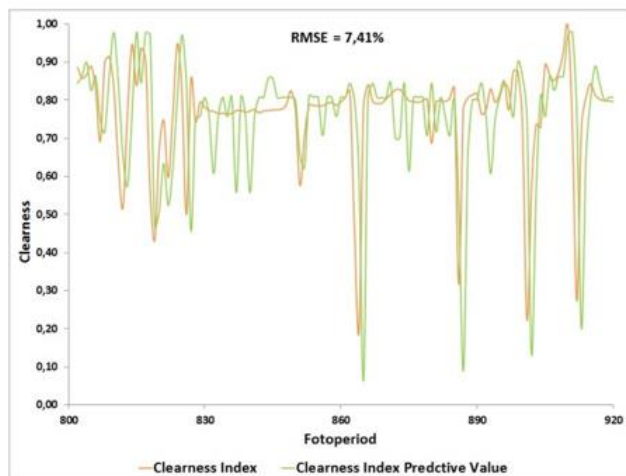


Figure 12. Ramp event occurrence - 09 January 2015

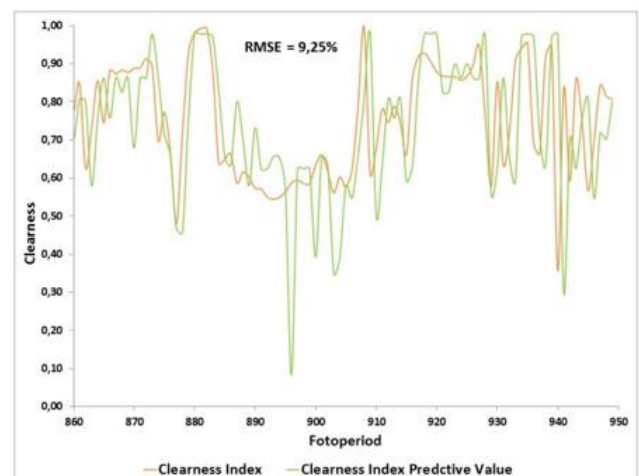


Figure 16. Ramp event occurrence - 15 January 2015

## 5.2. Tests for January 2016 Natal city data set.

In the same way, was applied the prediction approach implemented in MatLab, now for the year 2016, as can be seen in figures 24 to 39. The test for the days 03, 04, 05, 06, 07, 08, 09, 10, 11, 12, 13, 14, 17, 18 e 29 will not be presented as a function of the incidence profile of  $H$  have assumed a uniform distribution non-presenting the ramp events occurrences.

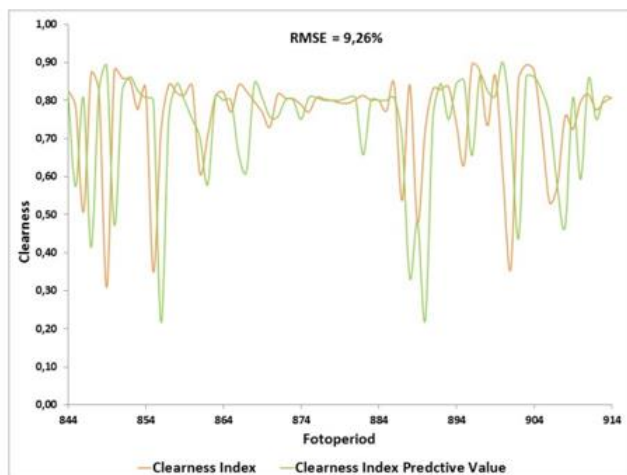


Figure 13. Ramp event occurrence - 10 January 2015

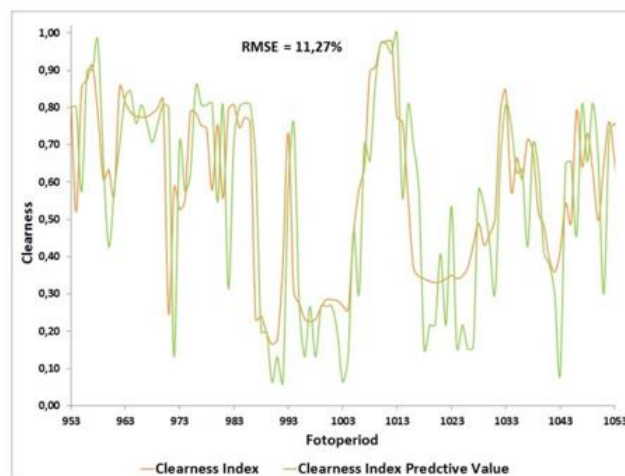


Figure 17. Ramp event occurrence - 17 January 2015

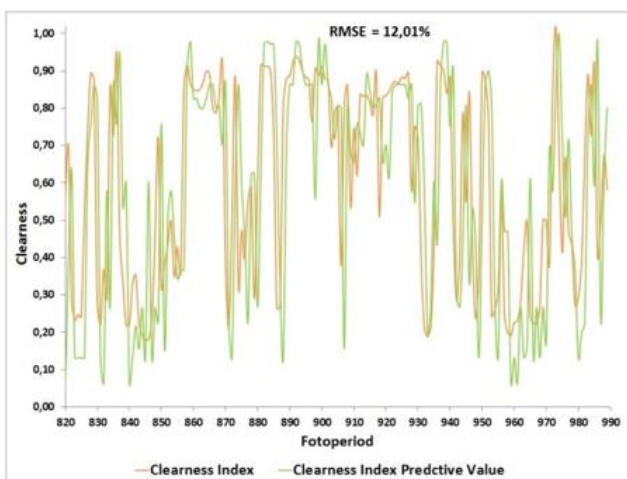


Figure 18. Ramp event occurrence - 11 January 2015

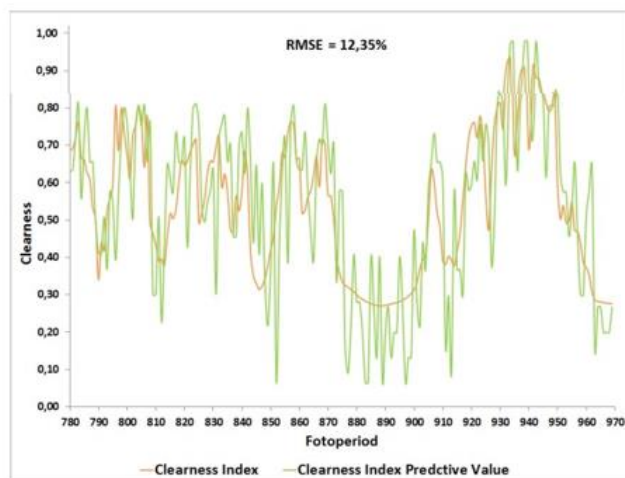


Figure 21. Ramp event occurrence - 23 January 2015

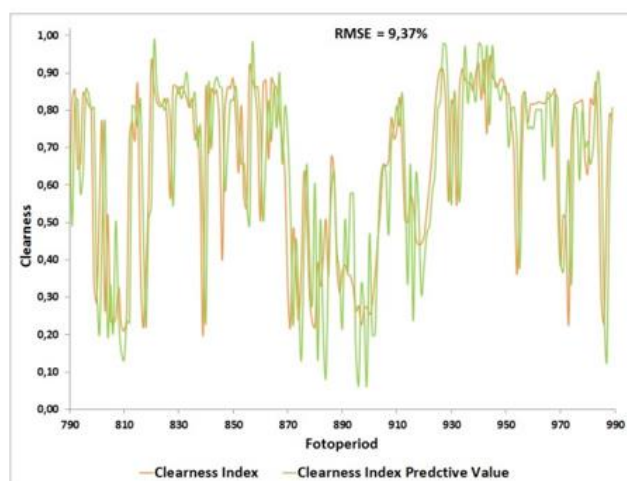


Figure 19. Ramp event occurrence - 19 January 2015

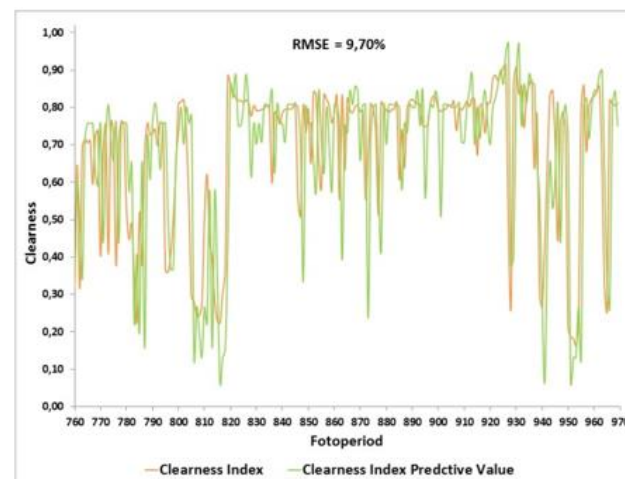


Figure 22. Ramp event occurrence - 24 January 2015

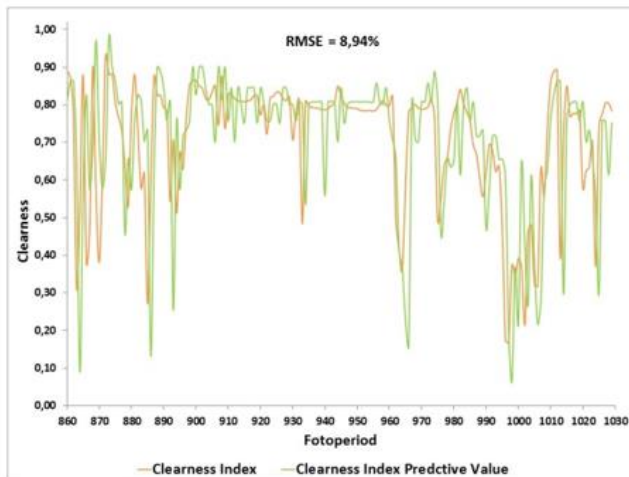


Figure 20. Ramp event occurrence - 22 January 2015

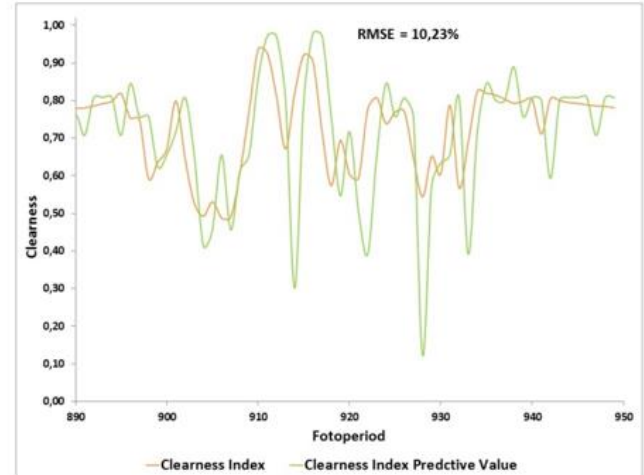


Figure 23. Ramp event occurrence - 31 January 2015

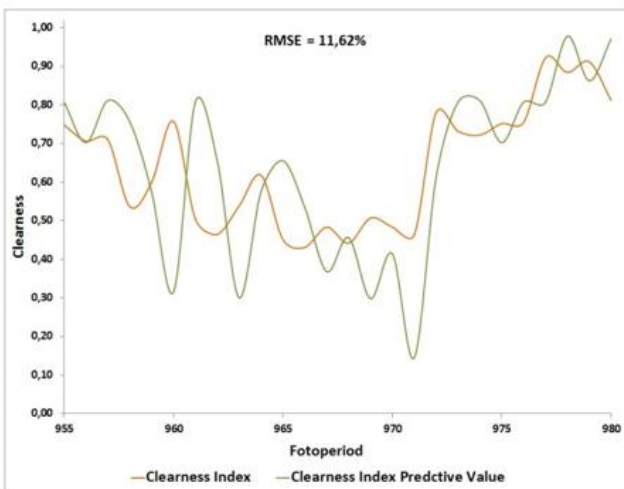


Figure 24. Ramp event occurrence - 01 January 2016

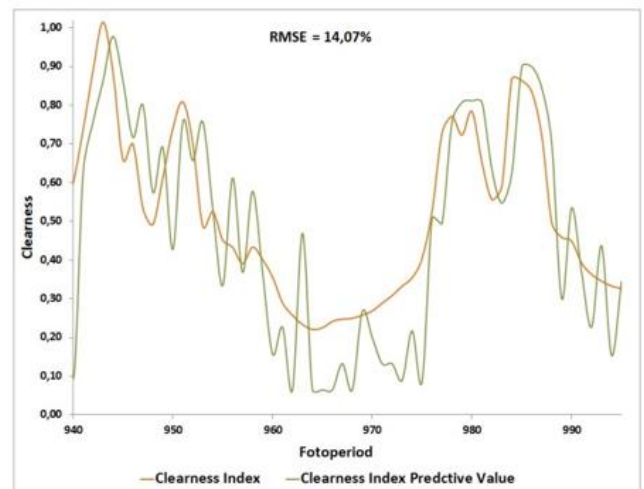


Figure 28. Ramp event occurrence - 19 January 2016

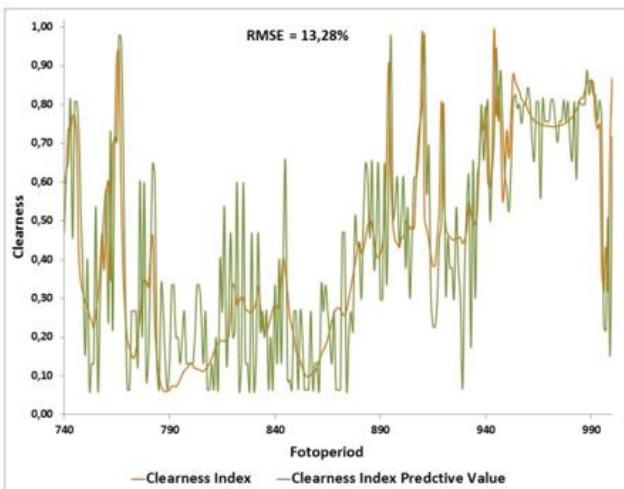


Figure 25. Ramp event occurrence - 02 January 2016

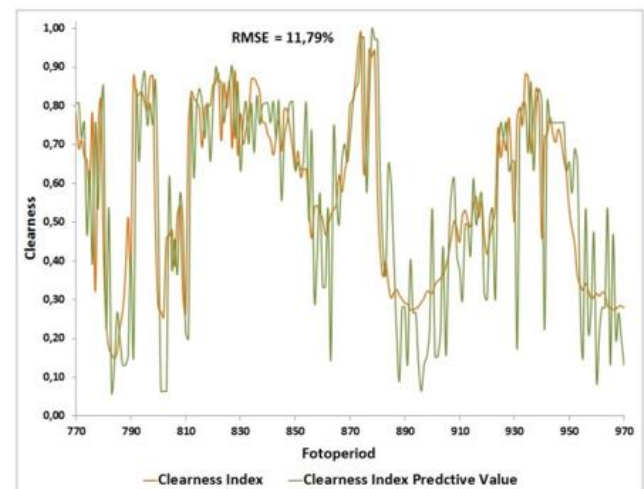


Figure 29. Ramp event occurrence - 20 January 2016

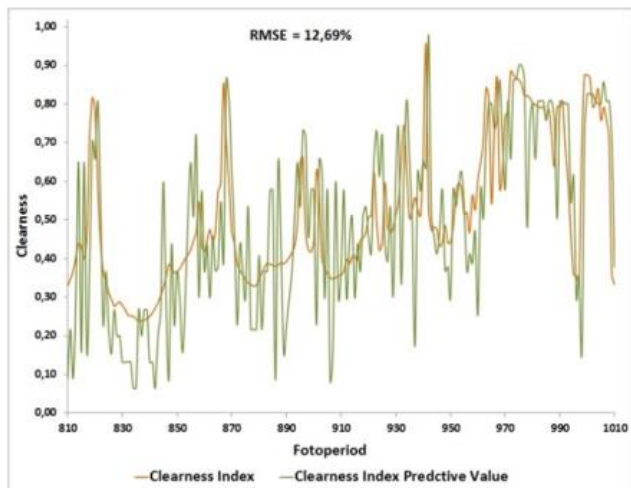


Figure 26. Ramp event occurrence - 15 January 2016

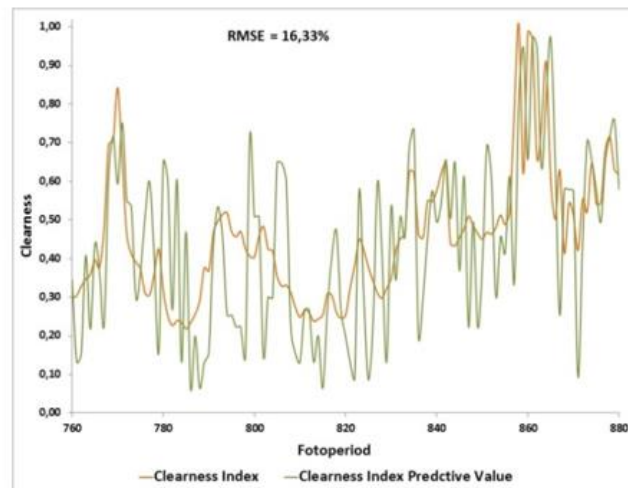


Figure 30. Ramp event occurrence - 21 January 2016

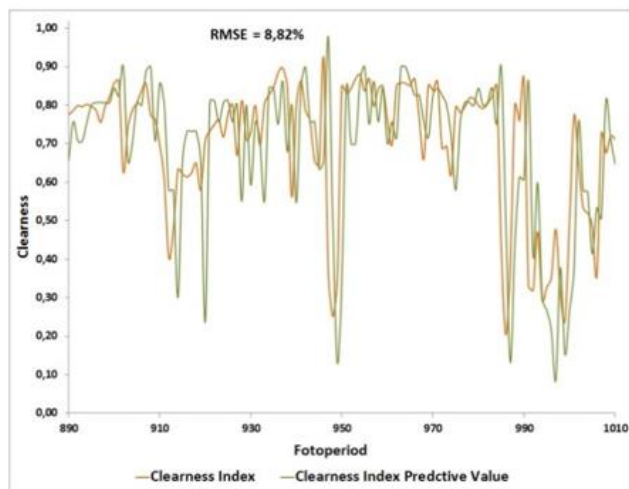


Figure 27. Ramp event occurrence - 16 January 2016

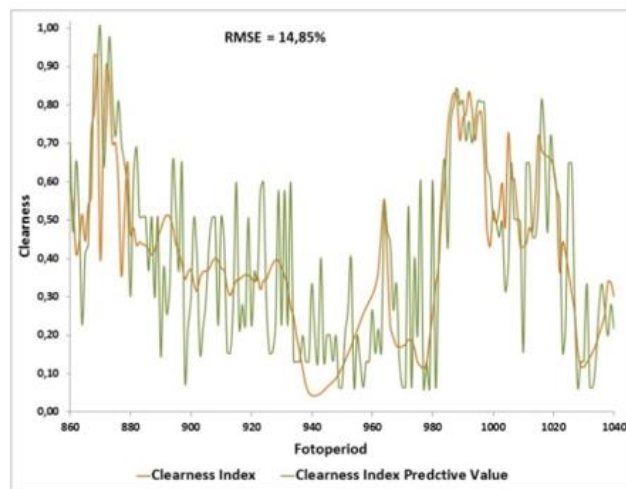


Figure 31. Ramp event occurrence - 22 January 2016

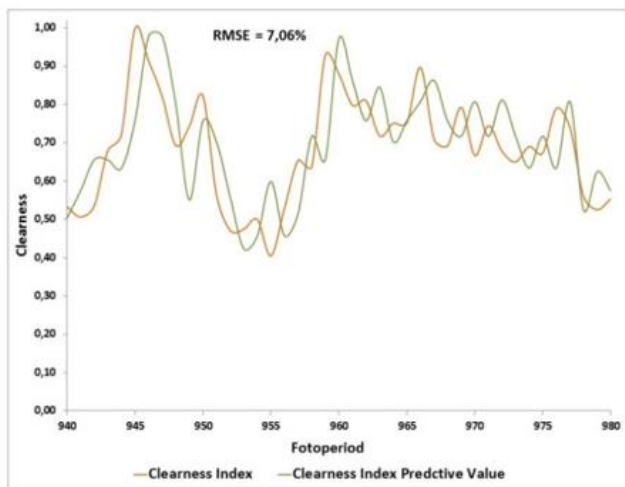


Figure 32. Ramp event occurrence - 23 January 2016

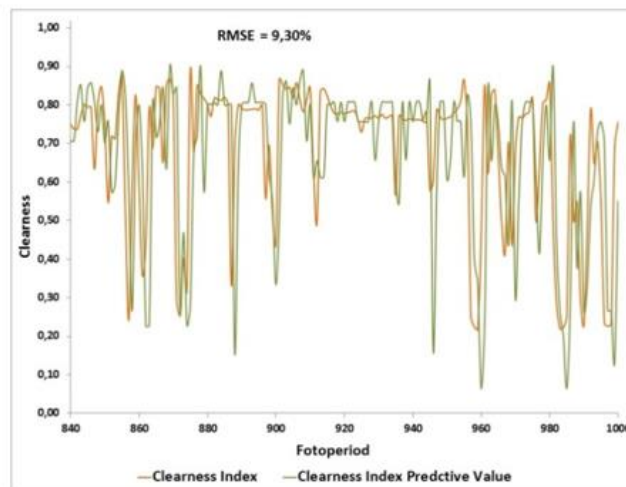


Figure 36. Ramp event occurrence - 27 January 2016

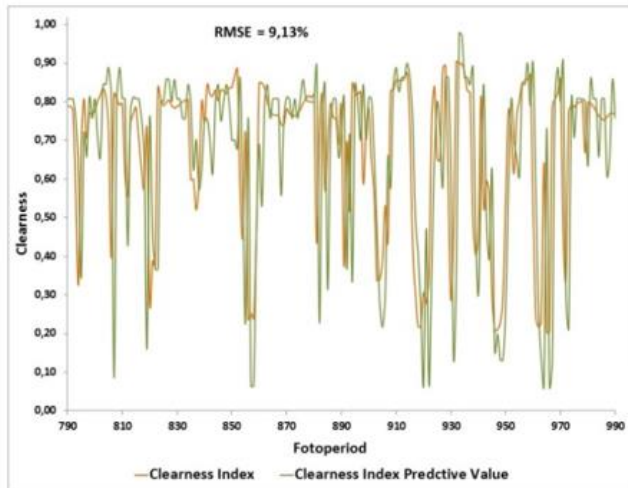


Figure 33. Ramp event occurrence - 24 January 2016

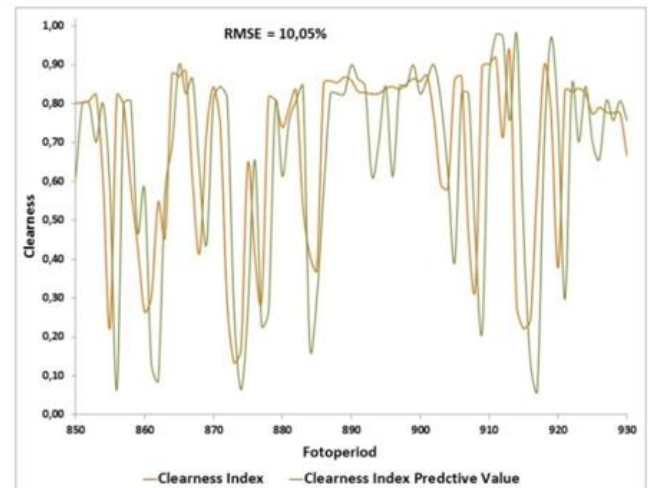


Figure 37. Ramp event occurrence - 28 January 2016

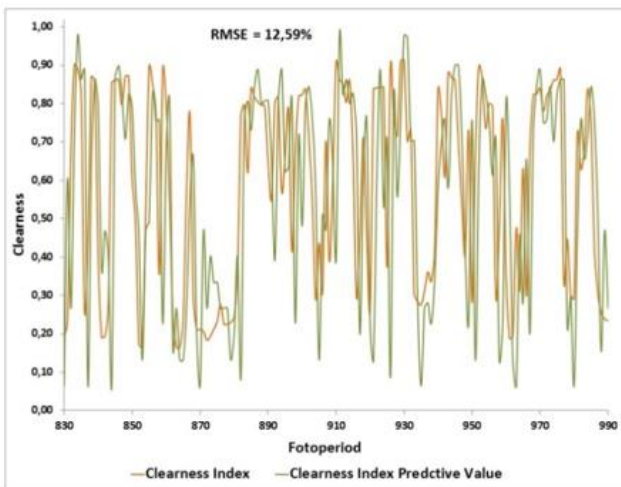


Figure 34. Ramp event occurrence - 25 January 2016

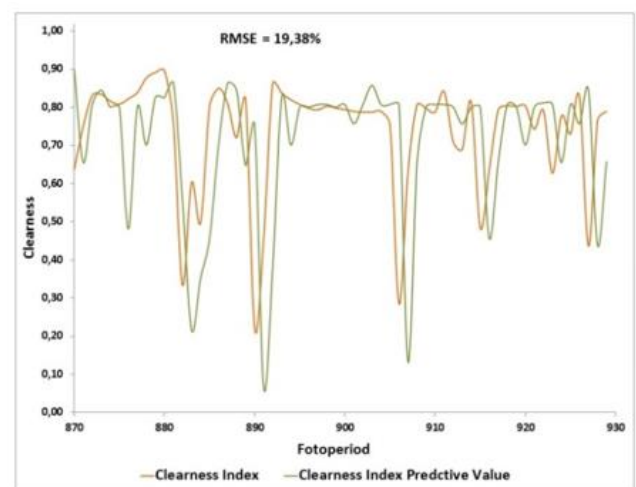


Figure 38. Ramp event occurrence - 30 January 2016

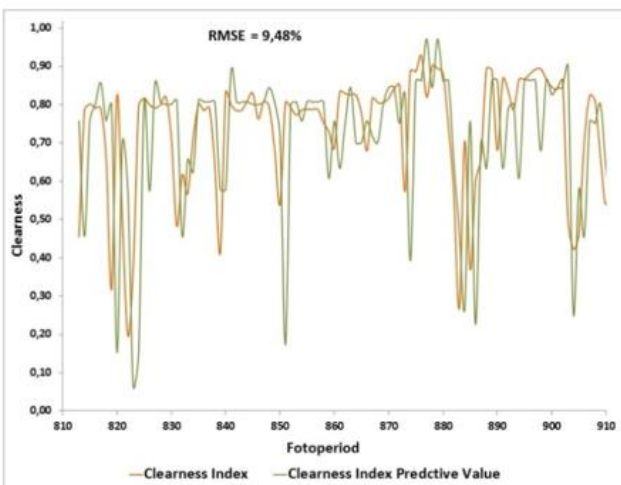


Figure 35. Ramp event occurrence - 26 January 2016

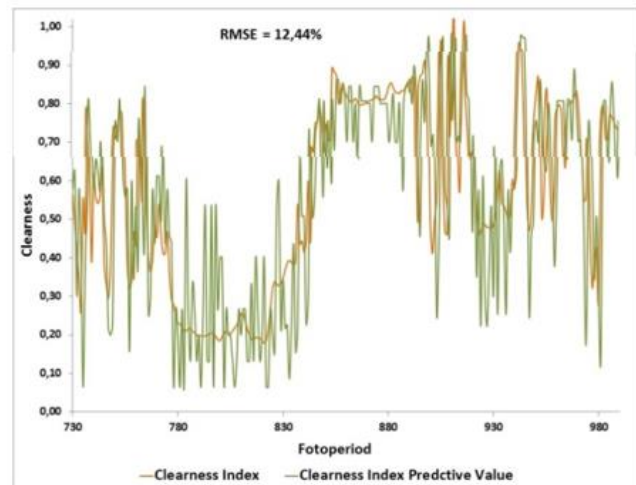


Figure 39. Ramp event occurrence - 31 January 2016

## 6. Results and discussion

According to proposed approach for evaluate the prediction performance was calculated parameters that quantify the degree of similarity between the calculated and predicted. In this context, time intervals were analyzed with short time from 12 minutes to 240 minutes, where it was possible to verify the performance of the probability transition matrix in the characterization of ramp events. When the time interval analyzed consider only the occurrence of ramp event, that is, the occurrence of periods of uniform distribution is null, or very small, a lower value is calculated by the RMSE, Indicating better precision in the prediction of global solar irradiance incidence, for the robustness test of the transition probabilities matrix, the following results can be summarized as below:

- Through the calculation results of RMSE for the tests of the solar data set referring to the January 2015 of Natal city, it was possible to establish a performance of the prediction method, at time intervals that presented ramp events, with an accuracy of 6,94% to 12,35% .
- Through the calculation results of RMSE for the tests of the solar data set referring to the January 2016 of Natal city, it was possible to establish a performance of the prediction method, at time intervals that presented ramp events, with an accuracy of 7,06% to 19,36% .

The results evidenced the precision in probabilistic forecast of the ramp event, intervals analyzed as figure 8 for example, attest the performance of the transition probabilities matrix, constructs by the proposed algorithm, based only on the present data, which will certainly be useful for the challenges in this field: (a) the absence of a long amount of solarimetric dates and clouds patterns information; (b) there is an of solarimetric dates and clouds patterns information availability, however, are local or regional information.

## 7. Conclusion

In this paper, an algorithm for development of transition probabilities matrices to predicting ramp events of global solar irradiance, based on Markov model is presented. Therefore, we can conclude, although it is important to verify the performance of the algorithm in the construction of transition probabilities matrices for others and larger solar data set, this algorithm can be useful and contribute to higher prediction accuracy and to improve the reliability to quantify the global solar irradiance incidence, in local site where there is the absence of a long amount of solarimetric dates and clouds patterns information, and can be absorbed by grid operations and the probabilistic forecasts for uncertainty management additional that is a key challenge as the penetration of photovoltaic solar generation continues to increase.

## Acknowledgment

The authors would like to thank the CAPES (Coordenação de Aperfeiçoamento de Pessoal de Nível Superior), CNPq (Conselho Nacional de Desenvolvimento Científico e Tecnológico), FAPESP (Fundação de Amparo à

Pesquisa do Estado de São Paulo), DECOM (Departamento de Comunicações), FEEC (Faculdade de Engenharia Elétrica e de Computação) and the UNICAMP (Universidade Estadual de Campinas).

## References

- Achleitner, S. et al. (2014) 'SIPs: solar irradiance prediction system', *IPSN-14 Proceedings of the 13th International Symposium on Information Processing in Sensor Networks*, Berlin, Germany, p-p. 225–236.
- Aguiar, R. and Collares-Pereira, M. (1992) 'TAG: A time-dependent, autoregressive, Gaussian model for generating synthetic hourly radiation', *Solar Energy*, Vol.49, No.3, pp. 167–174.
- Cai, D., Xie, T., Huang, Q. and Li, J. (2014) "Short-term Solar Photovoltaic Irradiation Predicting Using a Nonlinear Prediction Method", *IEEE PES General Meeting / Conference & Exposition*, National Harbor, MD, USA, p-p. 1-5.
- Ehnberg, J.S.G. and Bollen, M.H.J. (2005) "Simulation of global solar radiation based on cloud observations", *Solar Energy*, Vol.78, No.2, pp. 157–162.
- Huang, H., Xu, J., Peng, Z., Yoo, S., Yu, D., Huang, D. and Qin, H. (2013) "Cloud motion estimation for short term solar irradiation prediction", *IEEE International Conference on Smart Grid Communications, SmartGridComm 2013*, Vancouver, Canada, p-p. 696–701.
- Jaouhari, Z.E., Youssef, Z. and Lhoussain, M. (2015) "Cloud T racking from Whole-Sky Ground- based Images', *3rd International Renewable and Sustainable Energy Conference (IRSEC)*, Marrakech, Morocco, p-p. 1-5.
- Ji, W., Chan, C.K., Loh, J.W., Choo, F.H. and Chen, L.H. (2009) "Solar radiation prediction using statistical approaches", *7th International Conference on Information, Communications and Signal Processing (ICICS)*, Macau, China, p-p.1-5.
- Kalisch, J. and Macke, A. (2008) "Estimation of the total cloud cover with high temporal resolution and parametrization of short-term fluctuations of sea surface insolation", in *Meteorologische Zeitschrift*, Stuttgart, Germany, pp. 603–611.
- Kim, T.Y., Ahn, H.G., Park, S.K. and Lee, Y.K. (2001) "A novel maximum power point tracking control for photovoltaic power system under rapidly changing solar radiation", in *IEEE International Symposium on Industrial Electronics*, Pusan, KOREA, pp. 1011–1014.
- Lawrence, E.J. (2014) "Renewable Energy Integration: practical management of variability, uncertainty, and flexibility in power grids". Elsevier, San Diego, CA.
- Liu, B.Y.H. and Jordan, R.C. (1960) "The interrelationship and characteristic distribution of direct, diffuse and total solar radiation", *Solar Energy*, Vol.4, No.3, pp. 1–19.
- Lopes, M.G. (2015) "Análise dos impactos técnicos resultantes da variabilidade de geração de curto prazo de sistemas fotovoltaicos". UNICAMP, Campinas, SP.

- Loschi, H., J., Iano, Y., León, J., Moretti, A., Conte, F.D. and Braga, H. (2015) "A Review on Photovoltaic Systems : Mechanisms and Methods for Irradiation Tracking and Prediction", *Smart Grid and Renewable Energy*, Vol.6, No.1, pp. 187–208.
- Loschi, H.J. (2017) "Proposal of a global solar irradiance prediction complementary method for short-term, based on Markov processes". UNICAMP, Campinas, SP.
- Loschi, H.J., Ferreira, L.A.S., Iano, Y., Nascimento, D.A. Cardoso, P.E.R. Conte, F.D. and Carvalho, S.R.M. (2017) "EMC Evaluation of Off-Grid and Grid-Tied Photovoltaic Systems for the Brazilian Scenario", *Journal of clean Energy Tecnnologies*. Vol.6, No.2, p-p. 125-133.
- Marquez, R. and Coimbra, C.F.M. (2013) "Intra-hour DNI forecasting based on cloud tracking image analysis", *Solar Energy*, Vol. 91, No.1, pp. 327–336.
- Martins, F.R.A., Guarnieri, R., Chagas, R.C., Neto, S.L.M., Pereira, E.B., Andrade, E. and Thomaz, C. (2007) "Projeto Sonda – Rede Nacional de Estações para Coleta de Dados Meteorológicos aplicados ao Setor de Energia", *I Congresso Brasileiro de Energia Solar*. 2007, São Paulo, Brasil, p-p. 1-9.
- Naoto, K., Shun, M., Kazuma, K. and Masaki, S (2014) "Two-State Markov Model of Solar Radiation and Consideration on Storage Size", *IEEE Transactions on Sustainable Energy*, vol.5, No.1, pp. 171–181.
- Perez, R., Kivalov, S., Schlemmer, J., Hemker, K. and Hoff, T. (2011) "Parameterization of site-specific short-term irradiance variability", *Solar Energy*. Vol.85, No.7, pp. 1343–1353.
- Reno, M.J., Hansen, C.W. and Stein, J.S. (2012) "Global Horizontal Irradiance Clear Sky Models: Implementation and Analysis", SANDIA REPORT, Albuquerque, NM.
- Soares, D.S.F. (2014) "Impactos da Dinâmica Atmosférica na Flutuação de Potência em Usinas Fotovoltaicas", UFMG, Belo Horizonte, MG.
- Song, J., Krishnamurthy, V., Kwasinski, A. and Sharma, R. (2013) "Development of a Markov-Chain-Based Energy Storage Model for Power Supply Availability Assessment of Photovoltaic Generation Plants", *IEEE Transactions on Sustainable Energy*, vol.4, issue.2, pp.491-500.
- Tapakis, R.D. and Charalambides, A.G. (2013) "Monitoring Cloud Motion in Cyprus for Solar Irradiance Prediction", *Conference Papers in Energy*, Vol. 2013, Limassol, Cyprus, pp. 1–6.